A method of initialization for dynamical weather forecasting

By K. MIYAKODA and R. W. MOYER, *Geophysical Fluid Dynamics Laboratory, Environmental Science Services Administration, Washington, D.C.*

(Manuscript received October 18, 1966)

ABSTRACT

A new technique to solve the balance equation for a given geopotential field is tested. The technique may offer a substitute for conventional methods of solving the ω- and the ψ-equations. The non-filtered thermo-hydrodynamical equations are used as the basis, and the balance solution is obtained iteratively by filtering out the high-frequency modes through the use of the Euler-backward time differencing scheme.

The merit of this technique as compared to conventional methods is that equations which include complicated processes, such as friction or heating, can be treated without difficulty, and that the balanced solution thus obtained appears completely consistent with the prognostic equations. Furthermore, it is no longer necessary to artificially modify the observed geopotential as in conventional schemes, so as to meet the ellipticity condition of the differential equations.

1. Introduction

To perform a time integration of the thermo-hydrodynamical equations, initial conditions are needed for the geopotential, wind, temperature, vertical velocity and moisture. These conditions can, in principle, be obtained from the observed data. However, the data may not always be used directly as initial conditions, even if the forecasting domain is covered with a dense observing network. If the data are used directly, a short-period oscillation of motion is produced and its amplitude appears unrealistically large. This is partly due to some inaccuracy in the data and partly due to the incompleteness of the forecasting model.

In view of the fact that the amplitude of the observed gravitational oscillation is not large, it seems reasonable to adopt the solutions of the quasi-geostrophic "*balance*" equation in a broad sense as initial conditions. (Hinkelmann, 1951; Phillips, 1960). "Balance" means that the fluid is in a state such that its flow is always adjusted to the pressure field under the control of gravity and coriolis forces (Rossby, 1938; Charney, 1955).

Mathematically speaking, this condition is expressed by the relationship between the stream function and the geopotential on an isobaric surface. If both of these quantities are related to each other through a formula without including time derivatives of any quantity in explicit form, they are in the balance condition.

More specifically, the balance condition at a certain time is given by assuming that the first and second order time derivatives of divergence of the velocity are set to zero. As a matter of fact, the *ω-equation* (Sumner, 1950; Bushby, 1952; Hinkelmann *et al.*, 1952) and the *balance equation* in the narrow sense (this will hereafter be called the "*ψ-equation*," where ψ is the stream function) (Charney, 1955; Bolin, 1955) are derived under these assumptions (Refer to Jurčec, 1964, and Washington, 1964). Initialization has hitherto been done by solving these equations with respect to ω or ψ under a given geopotential ϕ.[1]

This method, however, has two difficulties. (1) To make the balance solution completely consistent with the forecasting equations, one must use a fairly complicated form of differential equations and then solve them with an elaborate iteration technique. In principle, it is not impossible, but very complicated. For instance, the *ω-equation* should contain the terms of the vertical derivative of vertical transport of vorticity, the twisting term of vorticity and also the heating term. Relating

[1] Fjørtoft (1962) obtained a kind of balance equation by assuming that higher order time derivatives of the wind speeds are zero.

to the *ψ-equation*, the wind velocity should be a function of the stream function as well as the velocity potential, and the equation should include the friction as well. It is difficult and tedious to solve this type of equations (for instance, Fjørtoft, 1962; Miyakoda, 1963).

(2) To solve the *ψ-equation* especially (Bolin, 1955; Shuman, 1957; Miyakoda, 1956; Arnason, 1958) one encounters the difficulty of the mixed type problem; that is, the differential equations appear hyperbolic in some regions, whereas they are elliptic elsewhere. To solve the *ψ*-equation by the conventional technique (except Fjørtoft's), *the observed field of geopotential* should be modified so as to satisfy the ellipticity condition. Otherwise there is a strong possibility that the solutions would not be determined uniquely.

The hyperbolicity is, of course, created by imposing the balance assumption, and in nature, some imbalance must exist. Artificial modification of the observed data is always undesirable. It is even more so if the purpose is merely to fulfil an artificial condition for which there is no satisfactory physical rationale.

So there is a need for a simple technique to solve the balance equation which eliminates the difficulties mentioned above. It is true that the iteration technique proposed by Fjørtoft (1962) is one method that satisfies these requirements. But we are now looking for a simpler method.

Recently a prediction experiment using real data with a primitive equation model was performed by Smagorinsky *et al.* (1965). Its results have revealed somewhat puzzling and yet very interesting information on the initialization. They found that some quantities are not important in determining the future evolution of the atmospheric motion. For instance, the horizontal patterns and quantitative amounts of precipitation appear roughly the same, irrespective of the initial condition of vertical velocity, provided that the other initial conditions, such as temperature and the non-divergent component of wind, are kept equal. Apparently, the vertical velocity grew quickly, even from a zero initial condition. (A Rossby number smaller than unity is probably required.[1])

The above result may have various implications. For one thing, it may suggest that the initialization of the vertical velocity is not needed because the prediction equation will take care of it. As a matter of fact, two forecasts, i.e., one with a certain value of initial vertical velocity and the other with zero initial vertical velocity, showed similar results for at least 5 days. There is, however, a possibility that the solutions would begin to depart from each other after 5 days. (Mintz and Krishnamurti's result suggests this departure.) If this is true, details of the initial conditions become important for longer predictions.[2] Apart from this problem, quite independently a method to obtain vertical velocity is needed for diagnostic studies.

The second point suggested by the prediction experiments is that, since a marching integration of the prognostic equations produces reasonable values of vertical velocity, an initialization method may be obtained by utilizing the above fact.

Meanwhile, an idea has been proposed by Matsuno (1966) to use a special time differencing scheme for the purpose of initialization. It is known that certain finite difference methods have the property of reducing the amplitude of the high-frequency oscillations of fast-moving mode as the time integration proceeds (Eliassen, 1963; Kurihara, 1965). In our case, however, we do not march ahead in time, but stay at the same time level, and iterate the computations until the velocity field attains its equilibrium state.

This paper is a report on an attempt to do this. In section 2 an explanation of the balance

---

[1] According to a personal communication from Y. Mintz and T. N. Krishnamurti of the University of California, Los Angeles, they have also carried out similar experiments based on the original ideas of Mintz (1963), and obtained a similar result. Using a two-level primitive equation model without an explicit water vapor variable, they made the general circulation experiment and then took the geopotential heights from the general circulation control experiment at a certain day, and computed, respectively, the geostrophic wind with a variable and constant coriolis parameter, and the linear balanced wind. Using each of these wind fields as the initial winds, numerical integration with the model for the next 5 or 6 days was performed. With all three of these initial winds there was remarkably close agreement with the control experiment, in the behavior of the surface pressure field and the upper level wind and temperature fields, up to about five days.

[2] However, there is another opinion that for a longer period the prediction of a dissipation system is probably indeterminate in detail and neither prediction could be correct. If we accept this opinion, details of the initial conditions may be irrelevant in a long term deterministic sense.

equations will be given, and taking a simple example of linear, viscous, barotropic equations, the techniques for solving the balance equations are discussed and the results of numerical tests are displayed. Sections 3 and 4 are devoted to the comparison of the present results with solutions obtained by conventional techniques, i.e., ψ- and ω-equations.

2. Demonstration of the initialization method for the linearized barotropic model

Example of the barotropic model

To begin with, let us take a simple example. The equations are linear, viscous, barotropic, i.e.,

$$\frac{\partial \mathbf{v}}{\partial t} + f\mathbf{k} \times \mathbf{v} = -\nabla\phi - \lambda\mathbf{v}, \tag{2.1}$$

$$\frac{\partial \phi}{\partial t} = -H\nabla \cdot \mathbf{v}, \tag{2.2}$$

where f is the coriolis parameter, $\mathbf{v}$ is the horizontal velocity vector, which consists of the x- and y-components, u and v, H is the product of the mean depth of the fluid and acceleration of gravity, ϕ is the perturbed geopotential of the fluid's surface, $\mathbf{k}$ is a unit vector directing upward, and λ is the friction coefficient. Now the problem is to solve $\mathbf{v}$ under a given ϕ.

First, these equations are approximated by finite difference both in time and space, i.e.,

$$\mathbf{v}^{(\tau+1)} - \mathbf{v}^{(\tau)} = -\beta\mathbf{k} \times \mathbf{v}^{(\tau)} - \gamma\nabla\phi^{(\tau)} - \mu\mathbf{v}^{(\tau)}, \tag{2.3}$$

$$\phi^{(\tau+1)} - \phi^{(\tau)} = -\gamma H\nabla \cdot \mathbf{v}^{(\tau)}, \tag{2.4}$$

where τ is the index for time level, $\beta = f\Delta t$, $\gamma = \Delta t/(2\Delta s)$, $\mu = \lambda\Delta t$, Δt is the time increment, and Δs is the grid size. Note that for the sake of simplicity, a forward difference formula has been used for finite time differencing. The space difference operator ∇ is defined by

$$\nabla_x\phi = \phi(i+1, j) - \phi(i-1, j),$$

$$\nabla_y\phi = \phi(i, j+1) - \phi(i, j-1),$$

and

$$\nabla \cdot \mathbf{v} = u(i+1,j) - u(i-1,j) + v(i,j+1) - v(i,j-1)$$

where i and j are the indices of grid points in the x- and y-direction, respectively.

To express the balance condition, we introduce the velocity potential χ, and put $(\partial\chi/\partial t)_{t_0} = 0$, where t_0 is the time we are concerned with. In finite difference, we have

$$\chi^{(\tau_0+1)} = \chi^{(\tau_0)}. \tag{2.5}$$

Hereafter, τ is used instead of τ_0 for the sake of simplicity. As is known, χ is in the relation as

$$\varepsilon\nabla^2\chi^{(\tau)} = \nabla \cdot \nabla^{(\tau)}, \tag{2.6}$$

and
$$\varepsilon\nabla^2\chi^{(\tau+1)} = \nabla \cdot \mathbf{v}^{(\tau+1)}, \tag{2.7}$$

where

$$\left.\begin{aligned} &\varepsilon = 1/(2\Delta s), \\ &\nabla^2\chi = \chi(i+2, j) + \chi(i-2, j) + \chi(i, j+2) \\ &\qquad + \chi(i, j-2) - 4\chi(i, j). \end{aligned}\right\} \tag{2.8}$$

It may be readily seen that the equations so far do not make a complete set, because there are seven unknowns, i.e., $u^{(\tau)}$, $v^{(\tau)}$, $u^{(\tau+1)}$, $v^{(\tau+1)}$, $\chi^{(\tau)}$, $\chi^{(\tau+1)}$, and $\phi^{(\tau+1)}$ and six equations, (2.3) $\sim$ (2.7) [(2.3) includes two equations]. The equations that we need include the higher order differences in time; i.e.,

$$\mathbf{v}^{(\tau+2)} - \mathbf{v}^{(\tau+1)} = -\beta\mathbf{k} \times \mathbf{v}^{(\tau+1)} - \gamma\nabla\phi^{(\tau+1)} - \mu\mathbf{v}^{(\tau+1)}. \tag{2.9}$$

We then assume that

$$\chi^{(\tau+2)} = \chi^{(\tau+1)}, \tag{2.10}$$

where
$$\varepsilon\nabla^2\chi^{(\tau+2)} = \nabla \cdot \mathbf{v}^{(\tau+2)}. \tag{2.11}$$

Note that the relation (2.10) corresponds to $(\partial^2\chi/\partial t^2)_{t_0} = 0$. There are now ten equations from (2.3) through (2.11) except (2.8), and ten unknown quantities.

The next problem is how to solve these equations, so, let us consider two iteration schemes denoted by A and B. It will be seen that Scheme A is divergent, and B is convergent. Yet it will be convenient to start with Scheme A for the sake of explanation.

A preliminary explanation of the method

To avoid confusion in the mathematical notation, we introduce the following:

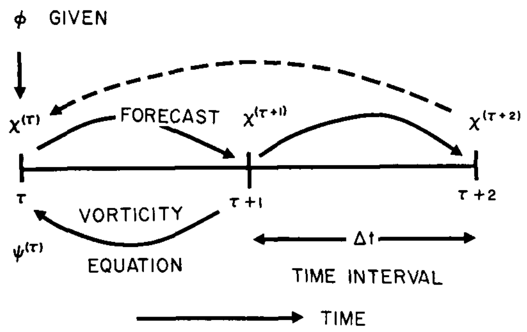

Fig. 1. Time levels and iteration scheme.

$$u_0 = u^{(\tau)}, \quad u_1 = u^{(\tau+1)}, \quad u_2 = u^{(\tau+2)},$$

$$v_0 = v^{(\tau)}, \quad v_1 = v^{(\tau+1)}, \quad v_2 = v^{(\tau+2)},$$

$$\phi_0 = \phi^{(\tau)}, \quad \phi_1 = \phi^{(\tau+1)}, \quad \phi_2 = \phi^{(\tau+2)}$$

$$\chi = \chi^{(\tau)} = \chi^{(\tau+1)} = \chi^{(\tau+2)}.$$

By so doing the index for the time level τ does not appear in the equations explicitly, and instead the iteration step ν will be used.

Iteration Scheme A

Equations (2.3), (2.4), and (2.9) are then written as

$$u_1^{(\nu)} = u_0^{(\nu)} + \beta v_0^{(\nu)} - \gamma \nabla_x \phi_0 - \mu u_0^{(\nu)}, \qquad (2.12)$$

$$v_1^{(\nu)} = v_0^{(\nu)} - \beta u_0^{(\nu)} - \gamma \nabla_y \phi_0 - \mu v_0^{(\nu)}, \qquad (2.13)$$

$$\phi_1^{(\nu)} = \phi_0 - \gamma H(\nabla_x u_0^{(\nu)} + \nabla_y v_0^{(\nu)}), \qquad (2.14)$$

and

$$u_2^{(\nu)} = u_1^{(\nu)} + \beta v_1^{(\nu)} - \gamma \nabla_x \phi_1^{(\nu)} - \mu u_1^{(\nu)}, \qquad (2.15)$$

$$v_2^{(\nu)} = v_1^{(\nu)} - \beta u_1^{(\nu)} - \gamma \nabla_y \phi_1^{(\nu)} - \mu v_1^{(\nu)}, \qquad (2.16)$$

where $u_0^{(\nu)}$, for instance, stands for the νth iteration of u_0.

The next step is to construct the formula to proceed from the νth to the $(\nu+1)$th iteration. This procedure should be designed in such a way that, in the final stage of the iteration, χ becomes equal for three time levels, i.e., τ, $\tau+1$, and $\tau+2$. In hope that convergence may be achieved, let us put (see Fig. 1)

$$\varepsilon \nabla^2 \chi^{(\nu+1)} = \nabla_x u_2^{(\nu)} + \nabla_y v_2^{(\nu)}. \qquad (2.17)$$

This means that the divergence at the νth iteration for the time level $\tau+2$ is equated to the divergence at the $(\nu+1)$th iteration for the time τ.

In this way, the procedure for getting the velocity potential has been set. As is known, wind vectors consist of the velocity potential χ as well as the stream function $\psi^{(\tau)}$. So we should have next the correction procedure for ψ. The scheme that we propose here uses the vorticity equation in reverse with time. Namely, taking cross-differences of equations (2.12) and (2.13), one may get the vorticity equation difference form, i.e.,

$$\nabla_x v_1 - \nabla_y u_1 = \nabla_x v_0 - \nabla_y u_0 - \beta \times (\nabla_x u_0 + \nabla_y v_0) - \mu(\nabla_x v_0 - \nabla_y u_0).$$

Now that the vorticity $\nabla_x v_0 - \nabla_y u_0$ is written as $\varepsilon \nabla^2 \psi$, the formula for ψ is given by

$$\varepsilon \nabla^2 \psi^{(\nu+1)} = \nabla_x v_1^{(\nu)} - \nabla_y u_1^{(\nu)} + \beta(\nabla_x u_0^{(\nu)} + \nabla_y v_0^{(\nu)}) + \mu(\nabla_x v_0^{(\nu)} - \nabla_y u_0^{(\nu)}). \qquad (2.18)$$

A computation based on this equation is a "*backward forecast*" or "*hindcast*."

We now have $\psi^{(\nu+1)}$ and $\chi^{(\nu+1)}$, so that $u_0^{(\nu+1)}$ and $v_0^{(\nu+1)}$ may be computed by formulas:

$$u_0^{(\nu+1)} = \varepsilon(-\nabla_y \psi^{(\nu+1)} + \nabla_x \chi^{(\nu+1)}), \qquad (2.19)$$

$$v_0^{(\nu+1)} = \varepsilon(\nabla_x \psi^{(\nu+1)} + \nabla_y \chi^{(\nu+1)}). \qquad (2.20)$$

Thus the equations from (2.12) through (2.20) constitute "*Iteration Scheme A*."

Convergence

Let us next examine the convergence of this scheme. For simplicity, an assumption is made on the spatial variation of the quantities. Suppose that all the quantities vary sinusoidally in the x- and y-direction. It then follows that, $\nabla_x \phi = k\phi$ and $\nabla_y \phi = l\phi$, where $k = 2\sqrt{-1}\sin(m\Delta s)$ and $l = 2\sqrt{-1}\sin(n\Delta s)$, m and n are the wave numbers in the x- and y-directions, respectively. Hence, $\nabla^2 \phi = (k^2 + l^2)\phi$.

By making use of these relations, the equations from (2.12) to (2.20) are rewritten. Then, insertions are repeated, and one ends up with

$$(k^2 + l^2) u_0^{(\nu+1)} = \xi_1 u_0^{(\nu)} + \xi_2 v_0^{(\nu)} + \xi_3 \phi_0, \qquad (2.21)$$

$$(k^2 + l^2) v_0^{(\nu+1)} = \eta_1 u_0^{(\nu)} + \eta_2 v_0^{(\nu)} + \eta_3 \phi_0, \qquad (2.22)$$

where, to save space, the descriptions of ξ and η are omitted.

Let us now denote the final solutions of $u_0^{(\nu)}$ and $v_0^{(\nu)}$ by u_0 and v_0, i.e., $u_0 = \lim_{\nu\to\infty} u_0^{(\nu)}$, $v_0 = \lim_{\nu\to\infty} v_0^{(\nu)}$, and the deviations of $u_0^{(\nu)}$ and $v_0^{(\nu)}$ from u_0 and v_0 by $\Delta u_0^{(\nu)}$ and $\Delta v_0^{(\nu)}$, respectively; for instance, $u_0 - u_0^{(\nu)} = \Delta u_0^{(\nu)}$.

It is then written that

$$(k^2 + l^2) u_0 = \xi_1 u_0 + \xi_2 v_0 + \xi_3 \phi_0, \tag{2.23}$$

$$(k^2 + l^2) v_0 = \eta_1 u_0 + \eta_2 v_0 + \eta_3 \phi_0, \tag{2.24}$$

and also

$$(k^2 + l^2) \Delta u_0^{(\nu+1)} = \xi_1 \Delta u_0^{(\nu)} + \xi_2 \Delta v_0^{(\nu)}, \tag{2.25}$$

$$(k^2 + l^2) \Delta v_0^{(\nu+1)} = \eta_1 \Delta u_0^{(\nu)} + \eta_2 \Delta v_0^{(\nu)}. \tag{2.26}$$

Equations (2.23) and (2.24) provide us with the final solutions if they converge. Equations (2.25) and (2.26) are the "*error equations*," which give the convergence rate of $u_0^{(\nu)}$ and $v_0^{(\nu)}$.

Eliminating $\Delta v_0^{(\nu)}$ and $\Delta v_0^{(\nu+1)}$ from (2.25) and (2.26), we have

$$(k^2 + l^2)^2 \Delta u_0^{(\nu+2)} - (k^2 + l^2)(\xi_1 + \eta_2) \Delta u_0^{(\nu+1)}$$
$$+ (\xi_1 \eta_2 - \xi_2 \eta_1) \Delta u_0^{(\nu)} = 0, \tag{2.27}$$

where

$$\xi_1 + \eta_2 = (k^2 + l^2)(1 + a_1),$$
$$\xi_1 \eta_2 - \eta_2 \eta_1 = (k^2 + l^2)^2 a_1,$$
$$a_1 = 1 - 2\mu + \beta^2 + \gamma^2 H(k^2 + l^2) + \mu^2 - 2\mu\beta^2.$$

Equation (2.27) is the transcendental equation for $\Delta u_0^{(\nu)}$. As is conventional in finite difference calculus, we put

$$\Delta u_0^{(\nu)} = \mathrm{X}^\nu, \tag{2.28}$$

ν in $\Delta u_0^{(\nu)}$ is the iteration step, but ν in X^ν is the exponent, and X itself is the convergence rate. Hence,

$$\mathrm{X}^2 - (1 + a_1)\mathrm{X} + a_1 = 0. \tag{2.29}$$

The solutions are: $\mathrm{X} = 1$ and a_1. The fact that one of the solutions is 1, means that the interative solution based on equation (2.28), does not converge.

Iteration scheme

As an alternative for Scheme A, we introduce the "*Euler-backward*" technique into this method for solving the balance equation. This name is suggested in Kurihara's paper (1965). Eliassen (1963) discussed the "*improved Euler-Cauchy*" method, which is slightly different from it, but is essentially the same. Also refer to Matsuno (1966).

This differencing technique is sometimes used to approximate first order time differential equations. The technique consists of two steps; namely, the "*Euler*" method which is virtually identical to the forward difference scheme, and the "*backward correction*". As mentioned earlier, the characteristic property of the Euler-backward method is that the high-frequency oscillation of the wave solution, such as the inertia-gravity wave, is gradually damped as the time integration proceeds. The damping effect is caused by the second step.

Iteration Scheme B

The application of the Euler-backward technique to the set of equations from (2.12) to (2.14) leads to:

$$u_1^* = u_0^{(\nu)} + \beta v_0^{(\nu)} - \gamma \nabla_x \phi_0 - \mu u_0^{(\nu)}, \tag{2.30}$$

$$v_1^* = v_0^{(\nu)} - \beta u_0^{(\nu)} - \gamma \nabla_y \phi_0 - \mu v_0^{(\nu)}, \tag{2.31}$$

$$\phi_1^* = \phi_0 - \gamma H(\nabla_x u_0^{(\nu)} + \nabla_y v_0^{(\nu)}), \tag{2.32}$$

and

$$u_1^{(\nu)} = u_0^{(\nu)} + \beta v_1^* - \gamma \nabla_x \phi_1^* - \mu u_0^{(\nu)}, \tag{2.33}$$

$$v_1^{(\nu)} = v_0^{(\nu)} - \beta u_1^* - \gamma \nabla_y \phi_1^* - \mu v_0^{(\nu)}, \tag{2.34}$$

$$\phi_1^{(\nu)} = \phi_0 - \gamma H(\nabla_y u_1^* + \nabla_y v_1^*). \tag{2.35}$$

Equations (2.30) to (2.32) correspond to the "Euler" method, and those from (2.33) to (2.35) to the "*Backward correction*" except the friction terms. u_1^*, v_1^*, and ϕ_1^* are quantities used only temporarily.

Equations (2.15) and (2.16) in Scheme A are modified in a similar way to be

$$u_2^* = u_1^{(\nu)} + \beta v_1^{(\nu)} - \gamma \nabla_x \phi_1^{(\nu)} - \mu u_1^{(\nu)}, \tag{2.36}$$

$$v_2^* = v_1^{(\nu)} - \beta u_1^{(\nu)} - \gamma \nabla_y \phi_1^{(\nu)} - \mu v_1^{(\nu)}, \tag{2.37}$$

$$\phi_2^* = \phi_1^{(\nu)} - \gamma H(\nabla_x u_1^{(\nu)} + \nabla_y v_1^{(\nu)}), \tag{2.38}$$

and

$$u_2^{(\nu)} = u_1^{(\nu)} + \beta v_2^* - \gamma \nabla_x \phi_2^* - \mu u_1^{(\nu)}, \tag{2.39}$$

$$v_2^{(\nu)} = v_1^{(\nu)} - \beta u_2^* - \gamma \nabla_y \phi_2^* - \mu v_1^{(\nu)}, \tag{2.40}$$

where ϕ_2^* corresponds to $\phi^{(\tau+2)}$, but it is used only as a carrying parameter.

The rest of the equations are exactly the same as in Scheme A, i.e., (2.17), (2.18), (2.19), and (2.20). So much for the procedure of Scheme B. Now the question might occur as to how the balance condition is satisifed in Scheme B. This point will be answered completely in the following discussion on convergence. But we mention now the following. Because of equation (2.17), $\chi^{(\tau)} = \chi^{(\tau+2)}$ will try to be achieved. Secondly, the Euler-backward technique is expected to give a timely smoothed solution. Combining these two points one can get eventually $\chi^{(\tau)} = \chi^{(\tau+1)} = \chi^{(\tau+2)}$, if the solution converges.

Convergence

Convergence of Scheme B can be examined analytically in a manner analogous to that in the previous section. Skipping the lengthy calculation, let us describe the final results. Corresponding to equations (2.21) and (2.22), we have

$$(k^2+l^2)u_0^{(\nu+1)} = \xi_1 u_0^{(\nu)} + \xi_2 v_0^{(\nu)} + \xi_3\phi_0, \quad (2.41)$$

$$(k^2+l^2)v_0^{(\nu+1)} = \eta_1 u_0^{(\nu)} + \eta_2 v_0^{(\nu)} + \eta_3\phi_0, \quad (2.42)$$

where

$$\left.\begin{aligned} \xi_1 &= a_1k^2 + b_1l^2 - \beta(a_2+b_2)kl,\\ \xi_2 &= \beta a_2k^2 - \beta b_2 l^2 + (a_1-b_1)kl,\\ \xi_3 &= \gamma(k^2+l^2)[(-1+a_3)k - \beta a_3 l], \end{aligned}\right\} \quad (2.43)$$

$$\eta_1 = \beta b_2k^2 - \beta a_2 l^2 + (a_1-b_1)kl,$$

$$\eta_2 = b_1k^2 + a_1l^2 + \beta(a_2+b_2)kl,$$

$$\eta_3 = \gamma(k^2+l^2)\,(\beta a_3 k + (-1+a_3)l),$$

and

$$a_1 = 1 - 3\beta^2 + \beta^4 + (3-2\beta^2)P + P^2 - 2\mu + 4\beta^2\mu - 3\mu P + \mu^2 - \mu^2\beta^2,$$

$$a_2 = 2 - 2\beta^2 + 2P - 4\mu + 2\mu\beta^2 - \mu P + 2\mu^2,$$

$$a_3 = -1 + 2\beta^2 - 2P + \mu - \mu\beta^2,$$

$$b_1 = 1 - \beta^2 + \beta^2 a_2,$$

$$b_2 = a_1 - 1 + \mu,$$

$$P = \gamma^2(k^2+l^2)H.$$

The equation of amplification factor X becomes,

$$X^2 - (a_1+b_1)X + a_1b_1 - \beta^2 a_2 b_2 = 0. \quad (2.44)$$

By solving this equation we conclude that scheme B is conditionally convergent. The convergence criterion for Δt is that, when $Q>0$ and $\lambda \neq 0$,

$$\Delta t < \frac{3(\hat{H}+f^2)(f^2+\lambda^2)}{\lambda f^2(2f^2+\lambda^2+\hat{H})}$$

or

$$\Delta t < \lambda^{-1},$$

where

$$\hat{H} = H[\sin^2(m\Delta s) + \sin^2(n\Delta s)]/\Delta s^2,$$

$$Q = \lambda^2\Delta t^2 + \lambda[2f^2 + 3\hat{H} - \lambda^2]\Delta t^3 + o(\Delta t^4).$$

And, if $\lambda = 0$, the criterion is given by

$$\Delta t < \sqrt{3}/\sqrt{f^2+H}, \quad \text{or} \quad \Delta t < 2/\sqrt{2f^2+3H}.$$

In the above pairs of inequalities for $\lambda \neq 0$ and $\lambda = 0$, the inequality with the smaller right hand term should be used. According to Matsuno (1966), the damping factor in the marching computation is the largest when $\Delta t \sim (1/\sqrt{2})F_{\max}$, where $F_{\max}$ is the maximum frequency of the solution. This information can be used in our problem.

Final solution of the iteration process when ϕ is a single Fourier component

The final solutions of $u_0^{(\nu)}$ and $v_0^{(\nu)}$ as $\nu \to \infty$ are derived from the equations similar to (2.23) and (2.24), i.e.,

$$u_0 = \left(-\frac{\gamma l}{\beta} - \frac{\gamma\mu l}{\beta}N + \gamma kN\right)\phi_0, \quad (2.45)$$

$$v_0 = \left(\frac{\gamma k}{\beta} + \frac{\gamma\mu k}{\beta}N + \gamma lN\right)\phi_0, \quad (2.46)$$

where

$$N = (-1 + a_2 + a_3)/(1 - a_1 - a_2\mu).$$

The first terms in u_0 and v_0 are the geostrophic components of wind. The first and the second terms are both rotational components, but the second term comes from the frictional effect. The third term is also due to friction, but it corresponds to the velocity potential.

Let us next investigate several important points concerning the solutions of u_0 and v_0. First, it is known that the balance condition is exactly satisfied; χ_0 corresponding to (u_0, v_0), (u_1, v_1) and (u_2, v_2) are equal to each other. Secondly, it is proven that the solutions of u_0 and v_0 fulfill the ψ-equation completely, which may be obtained by taking cross-differences of equations (2.12) and (2.13). Thirdly, u_0 for instance can be transformed to

$$u_0 = \left(-\frac{\hat{l}}{f} + \frac{\lambda^2}{\lambda^2 + f^2 + \hat{H}} \cdot \frac{\hat{l}}{f} - \frac{\lambda \hat{k}}{\lambda^2 + f^2 + \hat{H}} \right) \phi_0 + o(\Delta t),$$

where $\hat{k} = k/(2\Delta s)$, and $\hat{l} = l(2\Delta s)$. If Δt approaches zero, only the terms in parenthesis remain, and as it should be, u_0, u_1 and u_2 become equal to each other at that time. It may be interesting to compare these solutions with those of steady state equations for (2.1) and (2.2), i.e.,

$$u_e = \left(-\hat{l} \frac{f}{f^2 + \lambda^2} - \frac{\hat{k}\lambda}{f^2 + \lambda^2} \right) \phi_0.$$

Our solutions are, therefore, quite different from the steady state solutions so far as the functional forms are concerned.

From the foregoing, we may conclude that Iteration Scheme B is convergent for a suitably chosen Δt, and that the solutions thus obtained satisfy completely the balance conditions, and in general that they do not coincide with the usual steady state solutions.

Numerical tests

To insure convergence with Iteration Scheme B, and also to investigate some of the numerical aspects, tests were made with the linear, viscous, barotropic forecasting equations, i.e., (2.1) and (2.2). In practice, the finite difference equations (2.30)–(2.40) and (2.17)–(2.20) were used.

The mesh was 20×20 gridpoints in the x- and y-direction. The boundary conditions were that, on two lines of gridpoints surrounding the domain, the normal components of fluid velocity to the boundary lines are set zero. The convergence was judged by checking

$$\left.\begin{aligned} \left| u_0^{(\nu+1)} - u_0^{(\nu)} \right| < \delta, \\ \left| v_0^{(\nu+1)} - v_0^{(\nu)} \right| < \delta, \end{aligned}\right\} \qquad (2.47)$$

where δ is a prescribed small value.

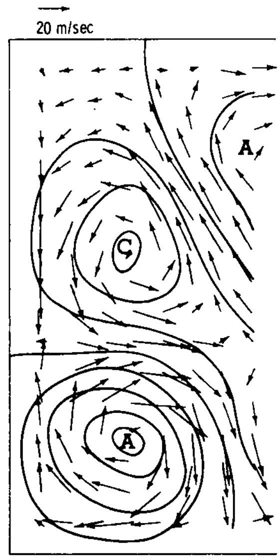

Fig. 2. The solution of the initialization is shown by the wind vectors at each gridpoint. The solid lines represent the original geopotential field. C is the center of cyclonic rotation and A is the center of anticyclonic rotation.

In practice, however, the iteration was carried out until the cycle number times Δt reached approximately half a day in real time; for instance, 144 iterations with $\Delta t = 5$ minutes. This indicates that the relaxation time for the solution to attain the equilibrium state is roughly half a day under normal meteorological conditions.

Results of computation

The constants used in the first experiment were: $f = 1.008 \times 10^{-4}$ sec^{-1}, $\lambda = 10^{-5}$ sec^{-1}, $H = 10^4$ m^2/sec^2, $\Delta t = 12$ min and $\delta = 0.01$ meter/sec.

Fig. 2 is the result, where the geopotential ϕ_0 originally given is indicated by the geostrophic streamlines, and the solutions are shown by arrows which are wind vectors. It is noticed, in the figure, that in the cyclonic area the wind vectors are slightly directed inward relative to the geostrophic streamlines, and in the anticyclonic area they are reversed. This is of course due to the friction effect.

In any case, the solution converges monotonically with iteration when Δt is less than the limit. Fig. 3 shows how the final solution varies with the magnitude of Δt. As is seen, if Δt is

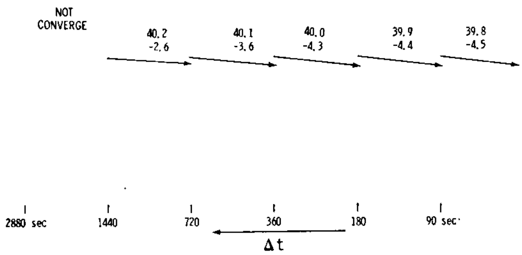

Fig. 3. Dependence of the final solution on Δt. Arrows indicate the solution of wind. Wind intensities of the x-component are shown by the upper figures, and of the y-component by the lower figures.

larger than 2880 sec, the solution does not converge. The dependence of the solution upon Δt is not large.

Laplacian computation

The Laplacian operator in finite difference for those in equation (2.17) or (2.18) was the formula (2.8). Let us denote it as ∇_A^2, and as an alternative, let us denote:

$$\nabla_B^2 R = R(i+1, j) + R(i-1, j) + R(i, j+1) + R(i, j-1) - 4 \cdot R(i, j), \tag{2.48}$$

where R is an arbitrary quantity.

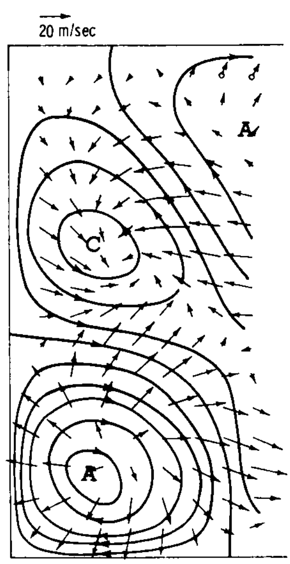

Fig. 4. The same as in Fig. 2 except this solution is wrong and is based on the inconsistent version of the finite difference Laplacian ∇_B^2. The correct solution based on ∇_A^2 is shown in Fig. 2.

It is very important to note that if ∇_x and ∇_y, as defined in section 2, are employed in computing $u_0^{(\nu+1)}$ and $v_0^{(\nu+1)}$ from ψ and χ, the use of the form ∇_B^2 is strictly prohibited. An inconsistent usage of ∇_B^2, ∇_x and ∇_y will result in a serious error as shown in Fig. 4. The correct solution corresponding to this is the pattern in Fig. 2, which was obtained from ∇_A^2. It may be seen that inconsistent application of the difference forms is like including fictitious friction.

Associated with the adoption of ∇_A^2, however, a two lattice separation of the solution, like a "*saw-tooth*" pattern, may be obtained. This point was mentioned by Bring & Charasch (1958) for the ψ-equation. The trouble is caused by improper prescription of two boundary conditions, i.e., the "physical" and "computational' conditions (Smagorinsky, 1958). But it can be reduced greatly by smoothing ϕ only near the boundary beforehand (see Fig. 5).

3. Application to the non-linear barotropic equations

Next, the initialization technique is applied to a slightly more complicated problem, which arises in the solution of the ψ-*equation*. The equation is derived from the barotropic equations, i.e.,

$$\frac{\partial \mathbf{v}}{\partial t} + (\mathbf{v} \cdot \nabla)\mathbf{v} + f\mathbf{k} \times \mathbf{v} = -\nabla\phi, \tag{3.1}$$

$$\frac{\partial \phi}{\partial t} + \nabla \cdot (\phi \mathbf{v}) = 0, \tag{3.2}$$

where f is assumed constant in space, and ϕ is the total geopotential height.

The iteration procedure for obtaining the balance solution for the system of equations (3.1) and (3.2) is set up in a way similar to the procedure in section 2.

Computed result and ψ-equation

Fig. 6 is an example of the solution for the case in which the space mean of ϕ is 6×10^4 m^2/sec^2 and $\Delta t = 360$ sec. It is interesting that there is wind divergence in the final solution, as shown in Fig. 6. This divergence is supposed to be a slowly changing component, although its intensity is extremely small: the maximum is 1/30 of f.

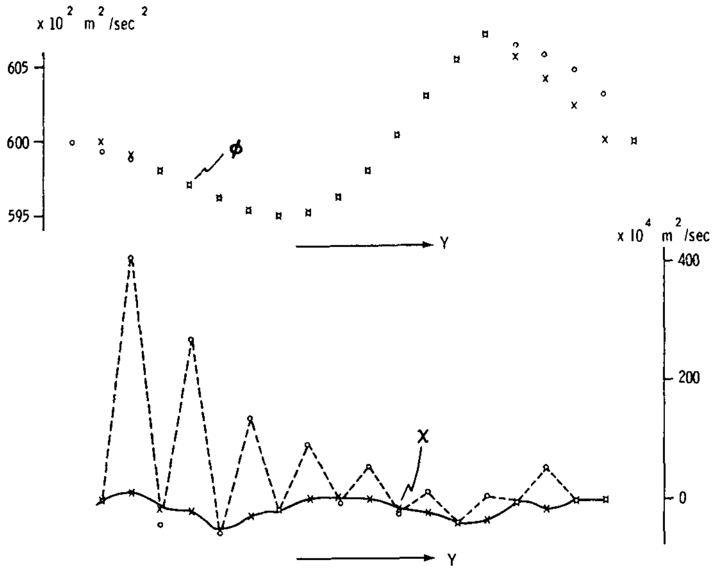

Fig. 5. The "saw-tooth" pattern created by solving the Poisson equation based on the Laplacian ∇_A^2 can be removed, to some extent, by smoothing the original geopotential field ϕ near the boundary. ϕ's marked by 0 in the upper figure are unsmoothed, and those marked by x are smoothed. In this case, ϕ was smoothed at 5 gridpoints from the boundary. The solutions of the velocity potential χ corresponding to the former are shown by 0, and those corresponding to the latter are indicated by x in the lower figure.

Let us next compare this solution with that of the conventional ψ-equation. As is known, assuming that $\partial\nabla^2\chi/\partial t = 0$, one gets from (3.1),

$$\frac{\partial}{\partial x}\left(u\frac{\partial u}{\partial x} + v\frac{\partial u}{\partial y}\right) + \frac{\partial}{\partial y}\left(u\frac{\partial v}{\partial x} + v\frac{\partial v}{\partial y}\right) - f\nabla^2\psi = -\nabla^2\phi. \tag{3.3}$$

If we further assume that $u = -\partial\psi/\partial y$ and $v = \partial\psi/\partial x$, and insert them into (3.3), the ψ-equation is obtained (Charney, 1955; Bolin, 1955),

$$2\left[\left(\frac{\partial^2\psi}{\partial x\partial y}\right)^2 - \frac{\partial^2\psi}{\partial x^2}\cdot\frac{\partial^2\psi}{\partial y^2}\right] - f\nabla^2\psi = -\nabla^2\phi. \tag{3.4}$$

It should be kept in mind that the solution of our balance equation does not necessarily satisfy (3.4), but it must satisfy (3.3). The numerical computation showed, however, that the values for wind as computed from the ψ-equation and from our equations were almost the same.

The mixed-type problem of elliptic and hyperbolic regions for the ψ-equation

Equation (3.4) becomes hyperbolic with respect to ψ if $\nabla^2\phi + f^2/2 < 0$. In this case, if the

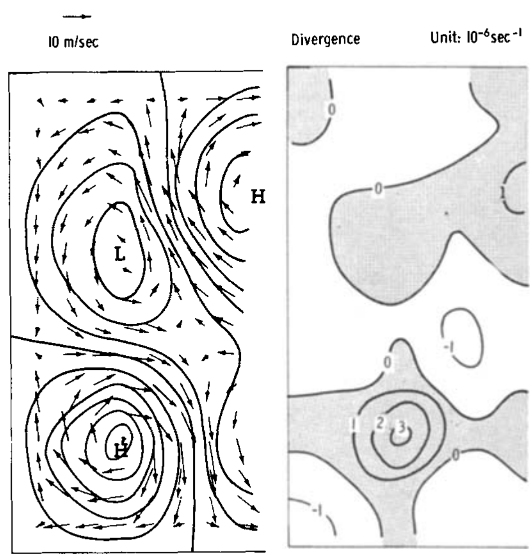

Fig. 6. The solution of the initialization for the divergent barotropic equation is shown by the wind vectors at gridpoints in the left hand side. The original geopotential field is indicated by solid lines. The distribution of wind divergence is shown on the right. Intensities are given in units of 10^{-6} sec^{-1}.

boundary condition is such that ψ is prescribed at all boundaries, the problem is not well posed. In practical computation, the solution does not converge by the conventional iterative method (except Fjørtoft, 1962). It is usual in such a situation to modify ϕ locally in such a way that hyperbolicity may be removed. This arrangement is, of course, unfavorable.

The present method has no difficulty in this respect. A solution can be obtained in any case, although the divergence appears very intense in hyperbolic areas. For example, it was 1/3 of the coriolis parameter in one of our examples in the hyperbolic areas. Note that the hyperbolicity condition for our equation has not yet been obtained; it is difficult because χ is also a function of ϕ.

4. Application to a two-level model

Finally we apply this method to a two-level linearized non-viscous baroclinic model. This experiment is especially useful, because a comparison can be made between the vertical velocity distribution obtained by the present method and the solution of the conventional ω-equation. Further, we took the vertical velocity computed at a certain time in the course of forecasting, and compared it with those of the balance solutions.

The model assumes basic flows at two levels, U_1 and U_2, and the perturbed flows are superimposed on them. The equations of motion are written as

$$\frac{\partial \mathbf{v}_k}{\partial t} + U_k \frac{\partial \mathbf{v}_k}{\partial x} + f\mathbf{k} \times \mathbf{v}_k = -\nabla \phi_k, \tag{4.1}$$

where k is the subscript for the vertical coordinate. The upper and the lower levels are indicated by $k = 1$ and $k = 2$, respectively. Using these numerical values for k, the thermal equation is:

$$\frac{\partial}{\partial t}(\phi_1 - \phi_2) + \bar{U} \cdot \frac{\partial}{\partial x}(\phi_1 - \phi_2) - f\Lambda(v_1 + v_2) - \hat{N} \cdot \omega = 0, \tag{4.2}$$

where $\phi_1 - \phi_2$ is the product of the acceleration of gravity and the thickness between two levels, $\hat{N}$ is the index of static stability, defined by $\hat{N} = \Delta P \cdot \partial\bar{\phi}/\partial P \cdot \partial \ln \bar{\theta}/\partial P$, θ is the potential temperature, ΔP is the pressure difference between the two levels, the bar notation is the space mean, $\bar{U}$ is the mean basic flow in the vertical defined by $\bar{U} = 1/2(U_1 + U_2)$, and Λ is the vertical shear of basic flow, i.e., $\Lambda = 1/2(U_1 - U_2)$.

The continuity equations are:

$$\nabla \cdot \mathbf{v}_1 + \omega/\Delta P = 0, \tag{4.3}$$

and

$$\nabla \cdot \mathbf{v}_2 - \omega/\Delta P = 0, \tag{4.4}$$

for the upper and the lower levels, respectively.

Forecasting

Using equations (4.1) to (4.4) and suitable initial conditions for u, v, ϕ, and $\omega(=0)$, forecasting was carried out for more than 5 days. The domain is a channel that is cyclic in the x-direction. The time differencing scheme is the Euler-backward method which suppresses the high-frequency mode of waves. At first we had adopted the usual centered time difference method, but the amplitude of the inertia-gravity wave was too large (see Matsuno, 1966) so we switched to the former. Fig. 7 is a result of forecast, where it is shown how the space mean of the absolute value of ω changes with time. It began at zero, increased rapidly at the beginning, and settled to an equilibrium value.

Now among these forecasts, we selected arbitrarily the 5th day as a sample of an equilibrium state. At this time, one can obtain ϕ and also ω (see Figs. 8 and 9). ϕ thus selected is used for the following computation, and ω will be used only for comparison.

ω-equation

If ξ denotes the relative vorticity and if we assume that $\xi = \nabla^2\phi/f$, it then follows that

$$\nabla^2\omega - b^*\omega + F = 0, \tag{4.5}$$

where

$$b^* = 2f^2/\Delta P \cdot \hat{N},$$

$$F = \frac{2\Lambda}{\hat{N}} \cdot \frac{\partial}{\partial x} \nabla^2(\phi_1 + \phi_2).$$

This is a simplified form of the ω-equation. ϕ_1 and ϕ_2 at the 5th day were inserted into F in the above equation, and the ω-equation was solved. The solution of quasi-geostrophic ω is displayed in Fig. 10.

In this particular case, ω's in Fig. 9 and 10 coincide with each other almost completely.

Present method

We now apply ϕ to the present initialization method. To do so, we must set up the finite difference equation. The details are omitted here.

Fig. 11 is the final solution of ω. By comparing this vertical velocity with those in Figs. 9 and 10, it may be said that they coincide rather well with each other, but in detail the pattern of Fig. 11 is shifted eastward by one gridpoint. This is really puzzling. We know from Kurihara's (1965) analysis of the Euler-backward method that the phase speed of a wave computed by this method will be greater than its real speed due to its aliasing error, so far as the centered space difference is adopted. With this information, our problem cannot be explained.

We have made a couple of attempts to avoid this discrepancy. In one attempt, the time levels used were shifted from the conventional system, i.e., τ, $\tau+1$, $\tau+2$ to a new one, i.e., $\tau-1$, τ, $\tau+1$ and ϕ was assumed to be given at τ. In this test the solution did not converge, however, probably because of an inappropriate iteration scheme. In a second attempt, a one sided space difference was used to approximate the advection term depending upon the sign (direction) of the advective flow. The solution did not differ significantly from the present one.

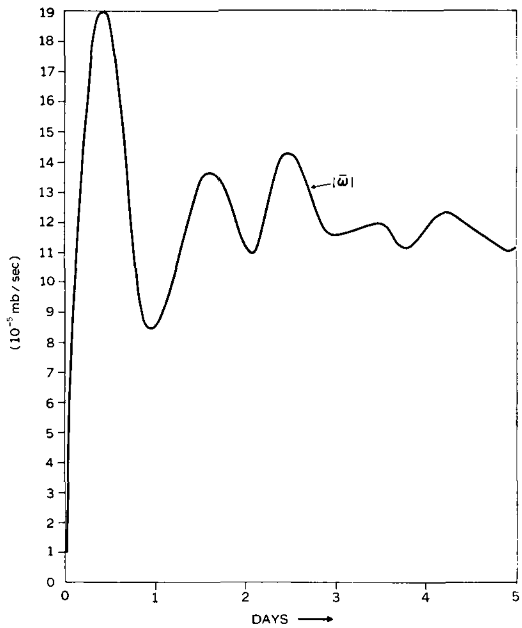

Fig. 7. Time evolution of the space mean of $|\omega|$.

Reduction of computation time

Most of the computation time is used in the relaxation of the Poisson equations, namely the equation for χ and for ψ. It is suspected that the

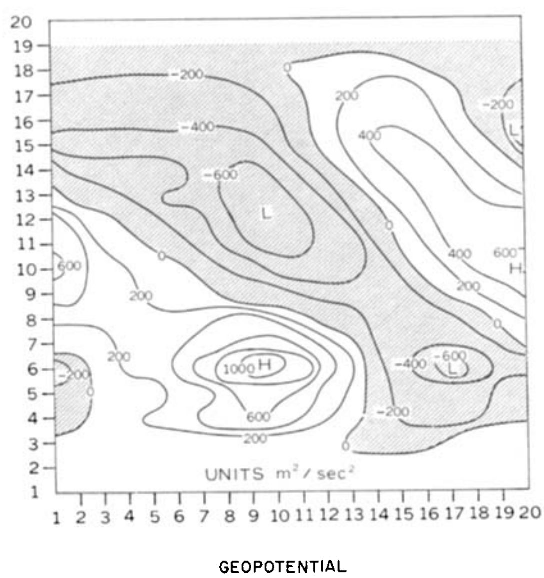

Fig. 8. Geopotential field ϕ at the upper level for the 5th day.

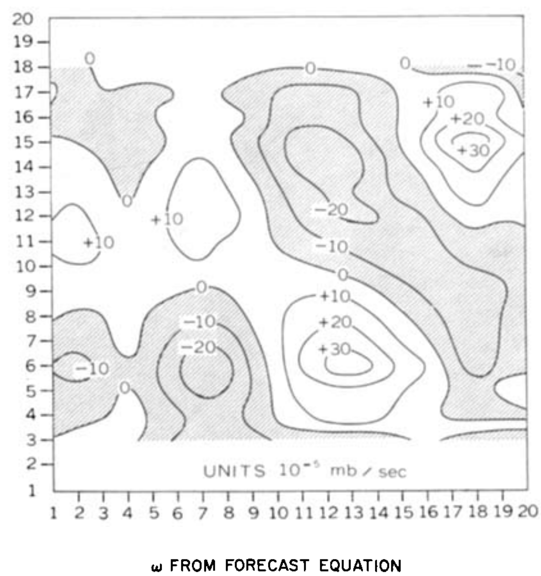

Fig. 9. ω computed in the prediction.

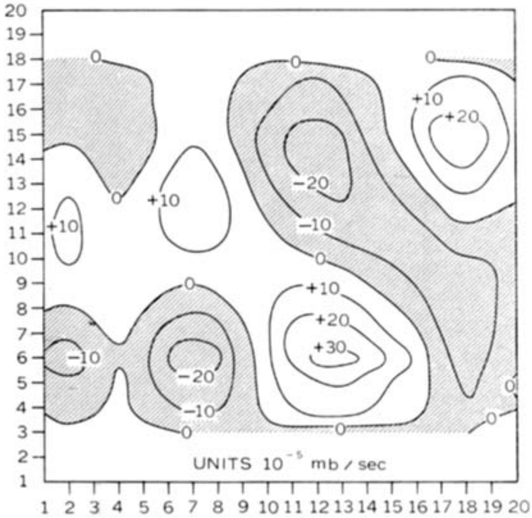

Fig. 10. ω computed by the ω-equation.

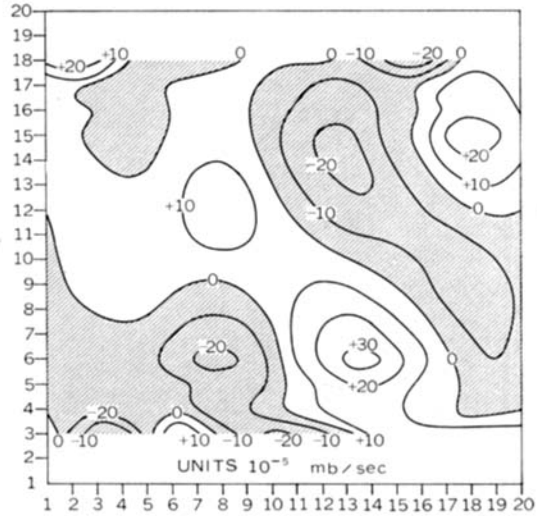

Fig. 11. ω computed by the present initialization method.

variation of ψ with each iteration is smaller than that of χ. Accordingly, ψ can be solved at infrequent intervals, whereas χ is solved every iteration.

Fig. 12 shows examples of the convergence of the solution, i.e., ω. The upper curve is for the version of skipping every two iterations, and the lower curve is for that of skipping every five iterations. Experiment shows that this kind of treatment saves time. But, as is seen in Fig. 12, the lower curve needs additional iterations in order to attain the final solution.

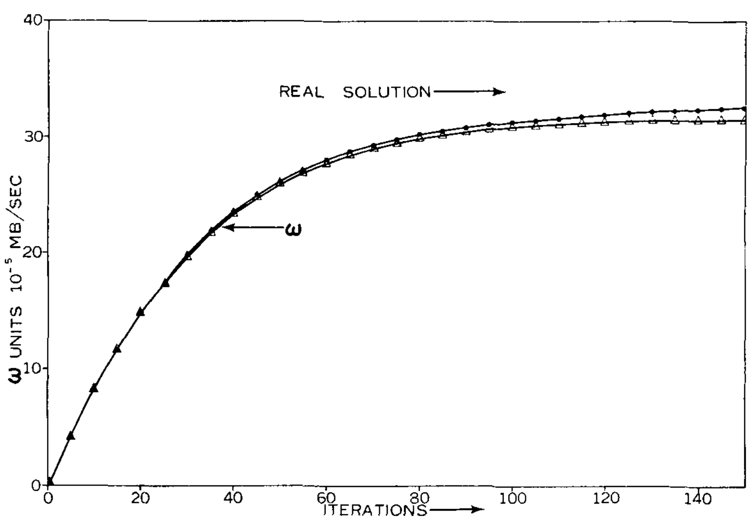

Fig. 12. Convergence of ω at a certain gridpoint. Δt is 720 sec. The upper curve shows the solution when the relaxation of ψ is skipped every two iterations. The lower curve shows a slower convergence when relaxation is computed every five iterations.

5. Conclusions and remarks

A technique to obtain the balance solution was discussed. The analytical study has proven that Iteration scheme B mentioned in section 2, which includes the "selective damping", is convergent if the time increment is properly taken.

The merit of this technique is that complicated effects can be included in the original equations, that is, the initialization scheme can be treated in almost the same degree of complexity as in a marching computation. The solution thus obtained is completely consistent with the prognostic equations. Furthermore, the artificial modification of observed data in the hyperbolic region is unnecessary.

The technique was applied to the non-linear viscous barotropic equations and to the linearized two-level non-viscous baroclinic equations. The solutions in the former problem compared well with those of the conventional ψ-equation. The test showed that a solution can be obtained even in the hyperbolic area for the ψ-equation, although the divergence of the wind is large.

In the latter problem, the vertical velocity obtained by the present method was compared to that obtained from the ω-equation. It was also compared to the vertical velocity computed in the forecast which was based on the non-filtered equations. Their distributions and intensities were roughly the same except that the pattern by the present initialization scheme was shifted slightly toward the east.

In conclusion, this initialization technique can be used to obtain the balance solution or the slowly changing component of the solution. There are, however, some defects in the method. The slight displacement of the vertical velocity pattern may be one of them. Another objection is that the scheme includes solving the Poisson equation which requires considerable computation time.

Acknowledgements

The authors are very grateful to Drs. S. Manabe and J. Smagorinsky for their advice and stimulating discussions. Special thanks are due to Mr. D. Hembree for carefully reading the manuscript. Many helpful comments on the first version of the manuscript were received from Drs. A. Arakawa, T. N. Krishnamurti and T. Matsuno, Professor Y. Mintz, Dr. W. M. Washington, and Dr. E. Rasmusson. Thanks are also due to Mr. T. Mauk for drawing the pictures and Mrs. R. Brittain, Miss M. Saffell, and Mrs. C. Bunce for typing the manuscript.

REFERENCES

Arnason, G. 1958. A convergent method for solving the balance equation. *J. Meteor. 15*, 220–25.

Bolin, B. 1955. Numerical forecasting with the barotropic model. *Tellus 7*, 27–49.

Bring, A. & Charasch, E. 1958. An experiment in numerical prediction with two non-geostrophic barotropic models. *Tellus 10*, 88–94.

Bushby, F. H. 1952. The evaluation of vertical velocity and thickness tendency from Sutcliffe's theory. *Quart. J. Roy. Meteor. Soc. 78*, 354–62.

Charney, J. G. 1955. The use of the primitive equations of motion in numerical prediction. *Tellus 7*, 22–26.

Eliassen, A. 1963. *On numerical integration of certain partial differential equations by means of the "Improved Euler-Cauchy Method"*. Tech. Note No. 1, Inst. of Theoret. Meteor., Univ. of Oslo, Norway, AFCRL-63-823.

Fjørtoft, R. 1962. A numerical method of solving certain partial differential equations of second order. *Geophys. Publ. Geophys. Norveg. 24*, 229–39.

Hinkelmann, K. 1951. Der Mechanisms des Meteorologischen Lärmes. *Tellus 3*, 285–96.

Hinkelmann, K., Essenwanger, O., Reymann, G. & Wippermann, F. 1952. Physicalisch-mathematische Grundlagen der numerischen Integration in einer baroclinen Atmosphäre. *Berichte des Deutsch.* Watt., US-Zone, No. 38, p. 416.

Jurčec, V. January, 1964. *Non-geostrophic vertical motions and energy transformations*. Ph.D. Dissertation, Univ. of California, Los Angeles.

Kurihara, Y. 1965. On the use of implicit and iterative methods for the time integration of the wave equation. *Mon. Wea. Rev. 93*, 33–46.

Matsuno, T. 1966. Numerical integrations of the primitive equations by a simulated backward difference method. *J. Meteor. Soc. Japan 44*, 76–84.

Mintz, Y. 1963. *Meteorological satellites and numerical weather prediction. The Application of Passive Microwave Technology to Satellite Meteorology*. A Symposium, RAND Corporation, Santa Monica, Mem. RM-3401 NASA, 1962.

Miyakoda, K. 1956. On a method of solving the balance equation. *J. Meteor. Soc. Japan 34*, 364–7.

Miyakoda, K. 1963. *Some characteristic features of winter circulation in the troposhere and the lower stratosphere*. Tech. Rep. No. 14, Dept. of Geophys. Sci., Univ. of Chicago.

Phillips, N. A. 1960. On the problem of initial data for the primitive equations. *Tellus 12*, 121–126.

Rossby, C. G. 1938. On the mutual adjustment of

pressure and velocity distribution in certain simple current systems. *J. Meteor. Res. 1*, 239–63.
Shuman, F. 1957. Numerical methods in weather prediction: I. The balance equation. *Mon. Wea. Rev. 85*, 329–32.
Smagorinsky, J. 1958. On the numerical integration of the primitive equations of motion for baroclinic flow in a closed region. *Mon. Wea. Rev. 86*, 457–66.
Smagorinsky, J., Strickler, R. F., Sangster, W. E., Manabe, S., Holloway, J. L. & Hembree, G. D. 1965. Prediction experiment with 9-level general circulation model. *Proceedings of the International Symposium on Dynamics of Large Scale Processes in the Atmosphere*, Moscow, USSR, 23–30, June 1965.
Sumner, E. J. 1950. The significance of vertical stability in synoptic development. *Quart. J. Roy. Meteor. Soc. 77*, 384–92.
Washington, W. M. 1964. *Initialization of primitive-equation models for numerical weather prediction.* Final Rep. (Part I) AFCRL-64-1005 (I) Contract No. AF 19(604)-7261, RT. Duquet, Project Director. Air Force Cambridge Research Laboratories, Office of Aerospace Research, USAF, Bedford, Mass.

МЕТОД ПОЛУЧЕНИЯ НАЧАЛЬНЫХ ПОЛЕЙ ДЛЯ ДИНАМИЧЕСКОГО ПРОГНОЗА ПОГОДЫ

Проверяется новая техника решения уравнения баланса для данного поля геопотенциала. Эта техника может заменить обычные методы решения ω- и ψ-уравнений. В качестве основы используются нефильтрованные термогидродинамические уравнения, и балансное решение получается итерационно путем отфильтровывания высокочастатных колебаний с помощью метода Эйлера с разностями по времени назад.

Достоинство данной техники по сравнению с существующими методами в том, что уравнения, которые включают такие сложные процессы, как трение и нагревание, могут быть легко исследованы, и получаемое таким образом балансное решение, по-видимому, полностью согласовано с прогностическими уравнениями. Кроме того, больше нет необходимости искусственно модифицировать наблюдаемый геопотенциал, как в обычных схемах, для удовлетворения условия эллиптичности при решении дифференциальных уравнений.